Cell PRESS
Open ACCESS

Cell Reports
Report

Structural Basis for Recognizing Phosphoarginine and Evolving Residue-Specific Protein Phosphatases in Gram-Positive Bacteria

Jakob Fuhrmann,[1,4] Beata Mierzwa,[2] Débora B. Trentini,[1] Silvia Spiess,[3] Anita Lehner,[1] Emmanuelle Charpentier,[3] and Tim Clausen[1,*]

[1]Research Institute of Molecular Pathology (IMP), A-1030 Vienna, Austria
[2]Institute of Molecular Biotechnology (IMBA), A-1030 Vienna, Austria
[3]The Laboratory for Molecular Infection Medicine Sweden, Umeå University, 90187 Umeå, Sweden
[4]Present address: Department of Chemistry, The Scripps Research Institute, Jupiter, FL 33458, USA
*Correspondence: clausen@imp.univie.ac.at
http://dx.doi.org/10.1016/j.celrep.2013.05.023

SUMMARY

Many cellular pathways are regulated by the competing activity of protein kinases and phosphatases. The recent identification of arginine phosphorylation as a protein modification in bacteria prompted us to analyze the molecular basis of targeting phosphoarginine. In this work, we characterize an annotated tyrosine phosphatase, YwlE, that counteracts the protein arginine kinase McsB. Strikingly, structural studies of YwlE reaction intermediates provide a direct view on a captured arginine residue. Together with biochemical data, the crystal structures depict the evolution of a highly specific phospho-arginine phosphatase, with the use of a size-and-polarity filter for distinguishing phosphorylated arginine from other phosphorylated side chains. To confirm the proposed mechanism, we performed bioinformatic searches for phosphatases, employing a similar selectivity filter, and identified a protein in *Drosophila melanogaster* exhibiting robust arginine phosphatase activity. In sum, our findings uncover the molecular framework for specific targeting of phospho-arginine and suggest that protein arginine (de) phosphorylation may be relevant in eukaryotes.

INTRODUCTION

Protein phosphorylation is a reversible posttranslational modification that is of paramount importance in regulating a variety of cellular processes including responses to environmental signals, metabolism, growth, and differentiation (Hunter, 1995). Protein phosphorylation is carried out by hundreds of different protein kinases that transfer the γ-phosphate from ATP to specific amino acids on proteins, predominantly to the side chains of serine, threonine, and tyrosine residues (Hanks and Hunter, 1995; Pereira et al., 2011). An arsenal of protein phosphatases counteracts this reaction by catalyzing the dephosphorylation of specific client proteins. Based on their sequence, structure, and function, protein phosphatases are grouped into three main classes. Phosphatases acting on phospho-serine/threonine (pSer, pThr) comprise the PPP (phospho protein phosphatase) and PPM (Mg^{2+}/Mn^{2+}-dependent protein phosphatase) families, whereas enzymes acting on phospho-tyrosine (pTyr) constitute the protein tyrosine phosphatase (PTP) superfamily (Barford et al., 1998; Stoker, 2005). In addition, specialized protein phosphatases act on phospho-aspartate, phospho-histidine, and phospho-cysteine residues (Klumpp and Krieglstein, 2009; Perego et al., 1994; Rigden, 2008; Sun et al., 2012). Given the excess of phosphorylated proteins, for example, about 50% of all eukaryotic proteins are phosphorylated once in their lifetime and about 30% of all human proteins are phosphorylated at any given time (Olsen et al., 2006), it is evident that the activities of protein kinases and phosphatases have to be carefully balanced to achieve the physiologically relevant phosphorylation level of targeted substrates.

Recently, an additional type of protein kinase was identified that targets arginine (Fuhrmann et al., 2009). This kinase, McsB, phosphorylates arginine residues in the winged helix-turn-helix domain of the transcriptional repressor CtsR, thereby preventing its binding to DNA and consequently inducing the expression of repressed genes. In vivo, its activity is counteracted by an annotated tyrosine phosphatase, YwlE (Elsholz et al., 2012). However, the precise molecular mechanism of this antagonistic effect is currently unknown. In contrast to the kinase, which is highly specific in modifying arginine residues (Fuhrmann et al., 2009), the substrate specificity of the YwlE phosphatase is controversially discussed. Whereas YwlE was initially described as having tyrosine phosphatase activity (Kirstein et al., 2005; Musumeci et al., 2005), a more recent analysis suggests that YwlE functions as an arginine phosphatase in vivo (Elsholz et al., 2012). Based on its amino acid sequence, YwlE belongs to the low-molecular-weight protein tyrosine phosphatase (LMW-PTP) family that has a conserved set of active-site residues (Zhang, 2003). For example, all LMW-PTPs have a specifically shaped binding pocket to distinguish pTyr from other phosphorylated residues. Given this conserved architecture, it is surprising that an annotated LMW-PTP appears to target a different phospho-residue. To clarify this point, we performed a

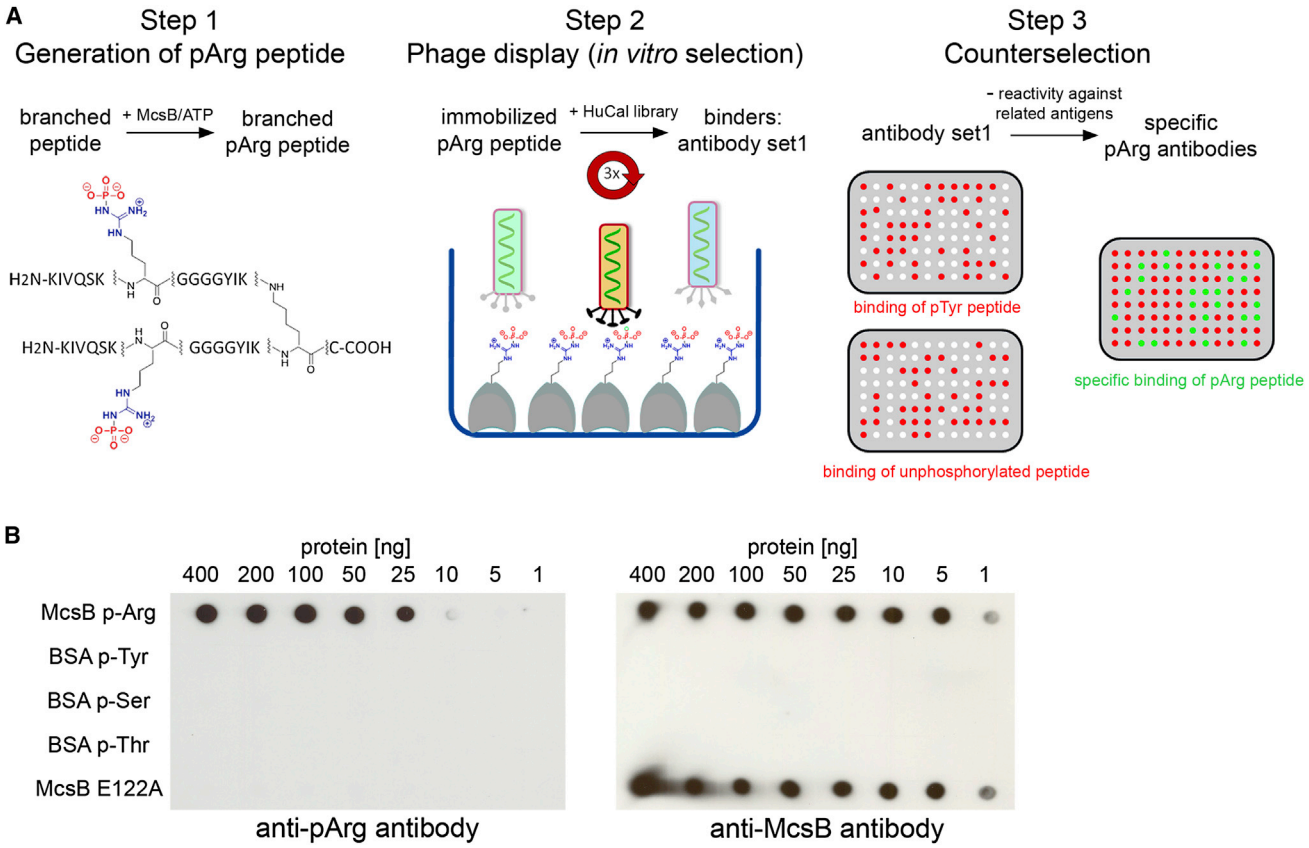

Figure 1. Generation of a pArg-Specific Antibody

(A) Schematic presentation of pArg antibody generation involving the enzymatic production of arginine phosphorylated peptide (step 1), selection of antigen-specific binders by phage display (step 2), and exclusion of cross-reactive binders by counterselection toward pTyr and nonphosphorylated peptides (step 3). (B) Dot-blot analysis highlighting the high specificity of the generated antibody in targeting the pArg-containing McsB protein (dilution of different proteins is indicated). The E122A mutant of McsB, which is catalytically inactive and thus cannot be autophosphorylated (Fuhrmann et al., 2009), was used as the non-phosphorylated control sample. The blot in the right panel was probed with a McsB-specific antibody yielding signals in both phosphorylated (McsB pArg) and unphosphorylated (McsB E122A) samples.

structural and biochemical analysis of YwlE from *Bacillus subtilis*. Using distinct phospho-peptide substrates, we show that YwlE is the founding member of a phosphatase family acting specifically on phosphorylated arginine residues. Crystal structures of YwlE reaction intermediates reveal molecular features that are essential to distinguish phospho-arginine (pArg) from other phospho-residues and ultimately led to the identification of a putative eukaryotic protein arginine phosphatase.

RESULTS

Generation of pArg-Specific Antibodies by an In Vitro Phage-Display Approach

To directly monitor the phosphorylation and dephosphorylation of arginine residues in bacterial cell lysates, we generated a pArg-specific antibody. Although we could produce pArg-containing proteins and peptides in large amounts, immunization trials carried out in various animal systems failed to produce a selective antibody. In contrast to O-linked phosphates such as pSer, pThr, and pTyr, free pArg has been described as an acid labile modification (Sickmann and Meyer, 2001). Presumably, it is this inherent lability of P-N linkages that caused problems in producing antibodies against pArg by classical immunization methods that rely on antigen internalization and processing in endosomal/lysosomal compartments under acidic pH conditions. Therefore, we switched to a defined in vitro methodology and applied, together with Morphosys AG, a specific phage-display approach at neutral pH (Prassler et al., 2011) (Figure 1A). For antibody screening, we used the branched phospho-peptide antigen (KIVQSKpRGGGGYIK)$_2$KC featuring two pArg residues. To remove cross-reactive antibodies, resulting phages recognizing the pArg peptide were further counterselected against the corresponding nonphosphorylated and pTyr-containing peptides (Figure 1A). The candidate pArg-specific binders were sequenced and subcloned into human $F_{(ab)2}$ antibody format. These antibodies were further selected by comparing their sensitivity of pArg recognition employing recombinant autophosphorylated McsB. Based on these data, we selected a single antibody for further characterizations. Ultimately, the specificity of the generated

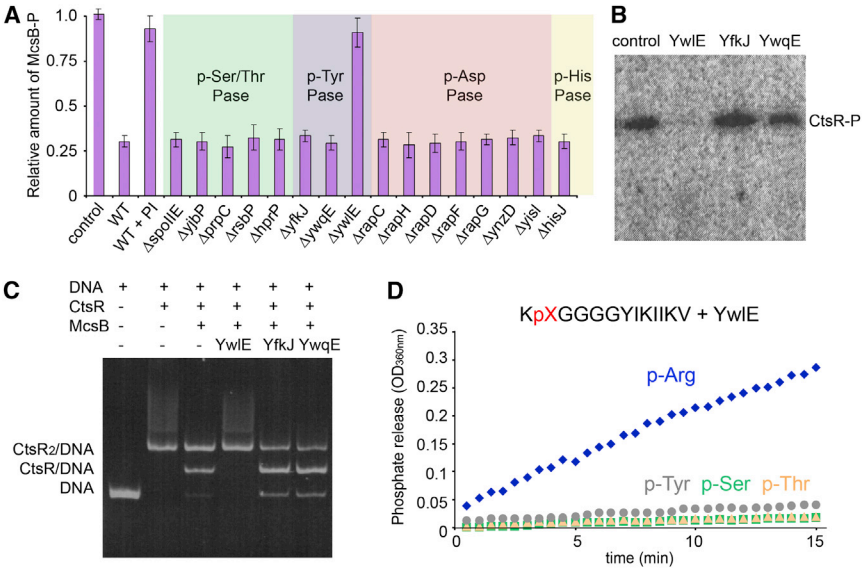

Figure 2. Characterization of the Protein Arginine Phosphatase YwlE

(A) ELISA-based screen monitoring the capabilities of different *B. subtilis* cell extracts to dephosphorylate a pArg containing substrate (McsB-P). The illustrated data are from three independent experiments performed in duplicates using wild-type (WT) and different phosphatase-deficient *B. subtilis* strains (disrupted genes indicated; PI, phosphatase inhibitors; Pase, phosphatase). Data are presented as mean ± SE.

(B) Autoradiogram of an SDS-PAGE gel of ^{32}P-labeled CtsR incubated with the recombinant phosphatases YwlE, YfkJ, and YwqE from *B. subtilis* (control, no phosphatase added).

(C) EMSA analysis monitoring the ability of CtsR to bind *clpC* promoter DNA. After preincubation with the protein arginine kinase McsB, various *B. subtilis* phosphatases were tested for their ability to restore the DNA-binding function of CtsR.

(D) Dephosphorylation of KpXGGGGYIKIIKV phospho-peptides. The pArg containing peptide was incubated with 5 nM YwlE, whereas all other phospho-peptides were treated with 20 μM YwlE.

recombinant pArg antibody was tested toward distinct phosphoproteins by dot-blot assays. For this purpose, pArg-containing McsB, pTyr BSA, pSer BSA, pThr BSA, and nonphosphorylated McsB were spotted onto a nitrocellulose membrane and incubated with the $F_{(ab')2}$ anti-pArg antibody. The resulting signals clearly indicated that the generated $F_{(ab')2}$ antibody is highly selective for pArg and does not cross-react with nonphosphorylated McsB or pTyr, pSer, or pThr proteins (Figure 1B). In sum, these findings demonstrate that the described phage-display methodology can be used to generate specific pArg antibodies in vitro. Given the chemical instability of the phospho-mark, it will be interesting to test whether this approach may be also applicable to raise antibodies against other acid labile posttranslational protein modifications such as pHis.

Characterization of YwlE as a Highly Specific pArg Phosphatase

Given the varying characterizations of McsB and YwlE as tyrosine and/or arginine directed enzymes (Elsholz et al., 2012; Fuhrmann et al., 2009; Hahn et al., 2009; Kirstein et al., 2005), we wanted to test whether the reported in vivo activity of dephosphorylating pArg-containing proteins is directly mediated by YwlE or a "side" reaction catalyzed by other *B. subtilis* protein phosphatases as well. Upon developing a pArg-specific antibody, we carried out ELISA screens to monitor the endogenous pArg phosphatase activity of various *B. subtilis* cell extracts. Using the autophosphorylated form of the protein arginine kinase McsB (McsB-P) as model substrate, we observed that a cell extract prepared from the *B. subtilis* wild-type strain had substantial pArg dephosphorylation activity, which was blocked by phosphatase inhibitors (Figure 2A). To pinpoint the responsible enzyme(s), we analyzed the pArg phosphatase activity of 16 *B. subtilis* mutant strains carrying chromosomal deletions of genes of all annotated protein phosphatases. These ELISA analyses revealed that the strain lacking YwlE was impaired in dephosphorylating McsB-P (Figure 2A), whereas cell lysates of the other phosphatase-deficient strains could not promote pArg dephosphorylation. Accordingly, YwlE should be the only active pArg phosphatase present in *B. subtilis*. To characterize this pArg phosphatase activity in vitro, we cloned and purified the three annotated *B. subtilis* tyrosine phosphatases YfkJ, YwqE, and YwlE and analyzed their ability to target the arginine phosphorylated CtsR (CtsR-P). Whereas recombinant YwlE efficiently removed the ^{32}P-labeled phosphate from CtsR-P within short time, CtsR-P was entirely resistant to dephosphorylation by YfkJ or YwqE (Figure 2B). Consistently, electrophoretic mobility shift assay (EMSA) studies showed that only YwlE can restore the DNA-binding ability of the repressor (Figure 2C) by reversing the McsB-mediated phosphorylation. Because YwlE was previously described as a tyrosine phosphatase, a classification mainly derived from sequence homology and the enzyme's activity against the general phosphatase substrate pNPP (Mijakovic et al., 2005), we next studied the activity against various peptide substrates containing different phosphoresidues embedded within the same sequence context (KpXGGGGYIKIIKV). Whereas the KpRGGGGYIKIIKV peptide was rapidly dephosphorylated, even at very low (5 nM) enzyme concentration, YwlE exhibited almost no activity against pSer, pThr, or pTyr peptides (Figure 2D). To rule out the possibility that unrelated phosphatases could have a similarly unpredicted arginine phosphatase activity, we tested different types of tyrosine, serine/threonine, and dual specificity phosphatases from different organisms in a pArg phosphatase assay (data not shown). Except for the promiscuous alkaline phosphatase, which showed about 15% of the YwlE activity, none of the enzymes was able to efficiently remove the phosphate group from the pArg peptide. Therefore, the dephosphorylation of pArg is not a general property or side reaction of other protein phosphatases. We conclude that YwlE is a highly specific protein arginine phosphatase (PAP) counteracting the McsB protein arginine kinase.

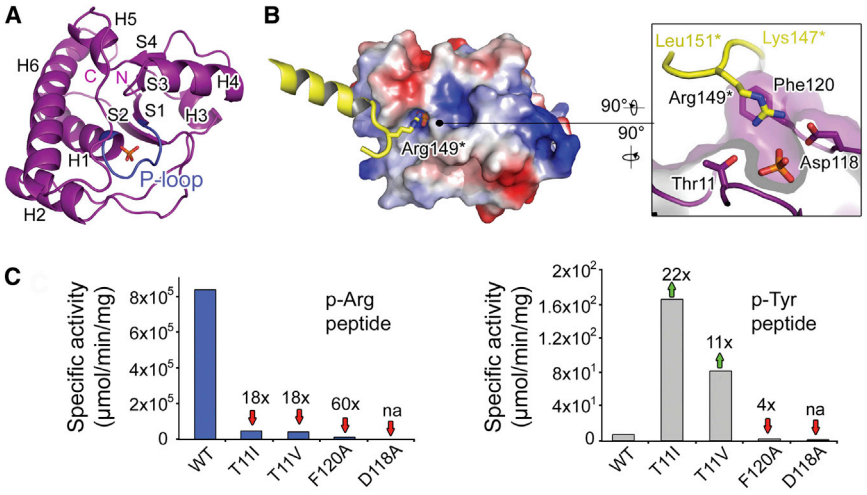

Figure 3. Active-Site Architecture of the YwlE Arginine Phosphatase

(A) Ribbon representation of YwlE with labeled secondary structural elements and highlighted P-loop (blue).

(B) Molecular surface of YwlE colored by its electrostatic potential. The C-terminal segment of a crystallographic neighbor is shown as a ribbon model (yellow) from where Arg149* protrudes into the active-site crevice (shown in closeup view in right panel).

(C) Mutational analysis of residues interacting with Arg149*. The panel represents the specific activity of distinct active-site mutants toward the pArg peptide (blue bars), whereas the right part depicts the specific activity against the corresponding pTyr peptide (gray bars). Additionally, an arrow above each bar highlights the relative increase or decrease in specific activity compared to the wild-type enzyme (na, no activity detectable).

See also Figure S1.

Crystal Structure of YwlE Capturing an Arginine Residue

Despite limited sequence similarity, all PTP enzymes share a seven residue CXXXXXR active-site loop region that comprises a conserved cysteine and arginine residue. This P-loop is critical for binding the phosphate group of the incoming substrate and subsequently, to form a transient enzyme-substrate phosphothioester adduct (Denu and Dixon, 1998). Unfortunately, neither detailed sequence analyses of PTP proteins nor the YwlE NMR structure (Xu et al., 2006), in which the active site is largely disordered, provides insight how to distinguish between pArg and pTyr substrates. To address this point, we determined the high-resolution crystal structure of YwlE from *B. subtilis* in its phosphate bound form (Table S1). Overall, YwlE adopts the typical LMW-PTP fold consisting of four β strands forming a central, highly twisted parallel β sheet that is flanked by helices H1, H2, H5, and H6 on one side, and H3 and H4 on the other side (Figure 3A). The P-loop encompassing the $C_7XXXXXR_{13}$ motif connects strand S1 and α helix H1 and constitutes the base of the active-site pocket. Here, residues Cys7 and Asp118 are properly arranged to dephosphorylate the incoming substrate in a concerted reaction (Zhang, 2003). The phosphate-binding site is formed akin LMW-PTPs by the side chain of Arg13, the backbone amides of the P-loop and the positive end of the macrodipole of helix H1, which together generate a highly positively charged pocket at the bottom of the substrate-binding cleft (Figures 3B and S1). Closer inspection of the active site revealed an additional electron density that could be unambiguously attributed to an arginine side chain that protrudes from a neighboring YwlE molecule in the crystal lattice (Arg149*), thus providing the unbiased view on the preferred YwlE ligand (Figure 3B). Remarkably, the loop segment harboring Arg149* adopts a similarly kinked conformation as the peptide ligand in the PTP1B phospho-substrate complex (Jia et al., 1995; Sarmiento et al., 2000) (Figure S1) implying that the observed crystal contact indeed reflects the interaction with a potential ligand. The substrate-mimicking Arg149* is sandwiched between Thr11, Asp118, and Phe120 with its guanidinium group hydrogen bonding to Asp118 (Figure 3B). To test the impact of Thr11, Asp118, and Phe120 on substrate specificity, we assayed the phosphatase activity of selected mutant proteins using pArg- and pTyr-containing peptides. Whereas mutating residues Asp118 and Phe120 almost completely abolished phosphatase activity, mutating residue Thr11 had opposing effects on the two substrates. Replacing Thr11 of YwlE by isoleucine resulted in significant reduction of pArg phosphatase activity while markedly increasing the activity toward the pTyr substrate (Figure 3C). The same effect was observed for the T11V mutation converting the YwlE arginine phosphatase into a better tyrosine phosphatase. Accordingly, substitution of a single hydroxyl group (threonine) by a methyl group (valine) or ethyl group (isoleucine) led to a drastic change in the substrate specificity of YwlE.

Structure of a Phospho-Enzyme Intermediate Reveals Details of pArg Recognition and Hydrolysis

The crystal structure of phosphate-bound YwlE provides a detailed view on the enzyme-product complex. To determine structural data of a distinct reaction intermediate illustrating how Thr11 directly interacts with the substrate's guanidinium group, we incubated several catalytically inactive YwlE mutants with the phosphorylated form of free arginine. By using the C7S mutant, we succeeded to obtain a complex, in which the chemically labile phosphate group of pArg was transferred to the introduced Ser7. The electron density map of the C7S mutant unequivocally reveals the formation of the covalent phospho-Ser7 adduct indicating that the crystallized mutant mimics the phospho-enzyme intermediate of the dephosphorylation reaction (Figure 4A). Interestingly, in the crystal structure of phospho-Ser7 YwlE, Arg149* moves 1.5 Å deeper into the substrate binding pocket such that its terminal nitrogens can form bidentate hydrogen bonds with the hydroxyl group of Thr11 and the carboxyl group of Asp118 (Figure 4A). Oriented by these residues, the angle formed by the η2 nitrogen atom of Arg149*, the phosphorus of the phosphate group and the hydroxyl oxygen of Ser7 is approximately 180° and thus consistent with a S_N2 nucleophilic substitution reaction, as outlined in Figure 4B. Accordingly, the C7S structure in complex with Arg149* highlights the

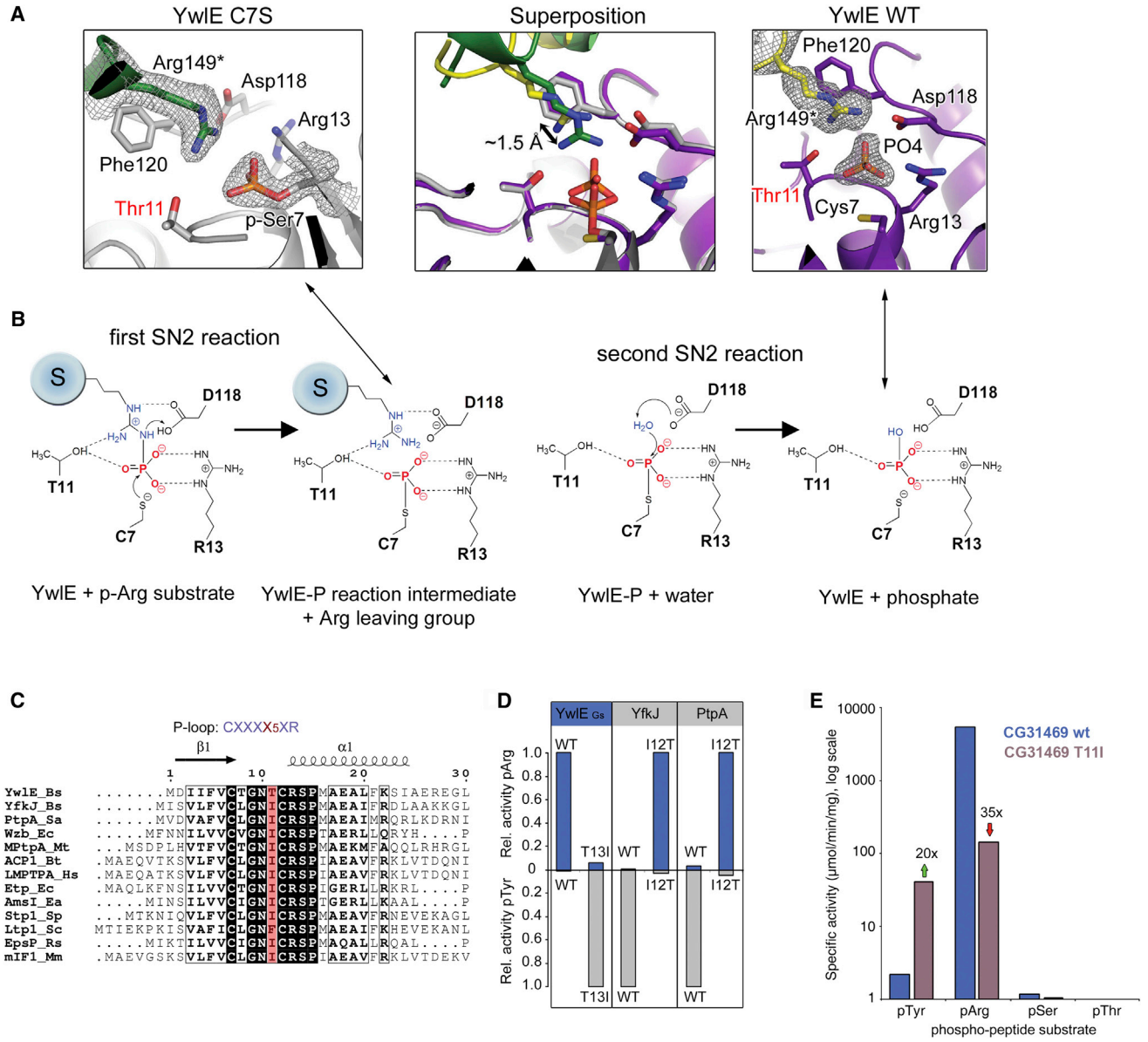

Figure 4. Structural Basis for Specifically Binding and Hydrolyzing pArg

(A) Active-site architecture of YwlE C7S mutant (left) and YwlE WT (right) reflecting the phospho-enzyme reaction intermediate and the enzyme-product complex, respectively (corresponding reaction intermediates indicated by arrows). The bound phosphate and Arg149* are overlaid with the 2FoFc omit electron density maps (contoured at 1.5 σ). The panel in the middle illustrates the superposition of the respective active sites.

(B) Supposed reaction mechanism of YwlE highlighting residues involved in substrate binding and catalysis. The structure of the phospho-C7S reaction intermediate supports a catalytic mechanism involving two sequential inline nucleophilic substitutions (SN) at the phosphorus. The first SN reaction is mediated by the thiolate of Cys7 that attacks the phosphorus atom of the incoming substrate, the second by an active-site water molecule that displaces the Cys7 thiolate, thus triggering phosphate release. Arg13 is critical for the coordination of the phosphate group (red), whereas residues Asp118 and Thr11 are crucial for precisely orienting the guanidinium group (blue) of the pArg substrate protein.

(C) Sequence alignment of the N-terminal segment of LMW-PTPs from various species. The PX5 residue of the conserved P loop is shaded in red.

(D) Substrate specificity of various PX5 mutants. The bars represent relative phosphatase activities toward pArg (up) and pTyr (down) peptide substrates.

(E) Activity of the putative *Drosophila* PAP. The bars represent the specific activity of CG31469 (blue) and its mutant version (CG31469 T11I, purple) toward pTyr, pArg, pSer, and pThr peptide substrates, respectively. The dephosphorylation activity was tested against the phospho-peptide ac-KpXGGGGYIKIIKV (pX denotes pTyr, pArg, pSer, or pThr).

See also Figures S2 and S3.

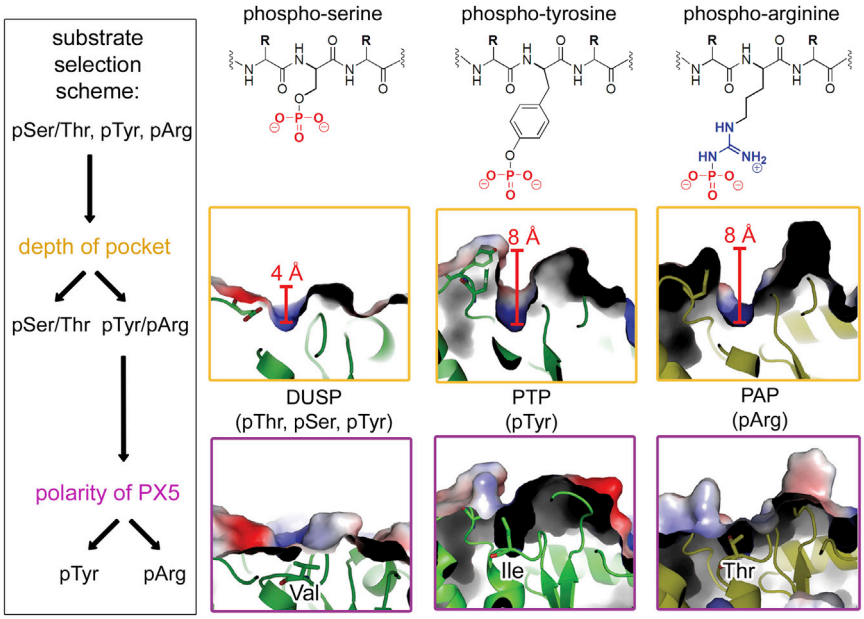

Figure 5. Determinants of Substrate Specificity within the LMW-PTP Family

Substrate selectivity against different phosphorylated residues is achieved by a two-step mechanism. First, phosphatases have evolved binding pockets of characteristic depth that reflects the size of their cognate substrates. The active-site clefts of PTPs (HPTP, Zabell et al., 2006) and PAPs (YwlE) are much deeper than those of the dual-specificity phosphatases (TMDP, Kim et al., 2007), which can dephosphorylate both pTyr and pSer/pThr residues (Patterson et al., 2009). Second, PAPs appear to have installed a polarity filter, Thr11, to detect the presence of the hydrophilic guanidinium group of the pArg substrate. Conversely, PTPs express an isoleucine as PX5 residue that contributes to the hydrophobic pocket accommodating the phenyl group of pTyr. See also Figure S3.

importance of Thr11 in binding the side chain of the incoming substrate, thereby ensuring the precise alignment of the phosphorylated guanidinium group for the dephosphorylation reaction.

Switching Phospho-Substrate Specificities by Mutating the PX5 Residue

Though all LMW-PTPs exhibit a similar active-site architecture, in which residues lining the substrate-binding cleft are particularly well conserved, structural comparison of YwlE with the related PtpA tyrosine phosphatase (Vega et al., 2011) reveals a remarkable difference regarding position 5 within the CXXXX$_5$XR P-loop (the PX5 residue; Thr11 in YwlE, Ile12 in PtpA) (Figure S2). As PX5 of YwlE directly interacts with the pArg substrate, tethering the guanidinium group adjacent to the phosphate group, the respective threonine-to-isoleucine exchange may have an immediate effect on substrate selection. Consistently, sequence analyses evaluating the conservation of the PX5 residue revealed that LMW-PTPs either express a hydrophobic residue (most often an isoleucine) or a threonine at this position (Figure 4C). Therefore, the PX5 residue may define the substrate specificity of the different phosphatase families. To test this idea, we generated Thr → Ile and Ile → Thr inversion mutants in PAP and PTP enzymes, respectively, and compared their activity with the wild-type proteins. Similarly as observed for the *B. subtilis* YwlE (Figure 3C), a Thr → Ile inversion in the PAP from *Geobacillus stearothermophilus* strongly diminished the hydrolysis of pArg substrates and markedly increased the pTyr phosphatase activity (Figure 4D). In analogy, the Ile → Thr exchange drastically improved the pArg phosphatase activity of the PTPs YfkJ or PtpA, while weakening their pTyr phosphatase activity. The effect of the Thr ↔ Ile mutations on substrate selection was further confirmed by analyzing the dephosphorylation of the pTyr mimicking compound para-nitrophenylphosphate (pNPP; Table S2). Derived kinetic parameters indicated that the PX5 mutation affects both the K_M (substrate binding) and the k_{cat} (orienting substrate for catalysis) of the dephosphorylation reaction. In sum, these findings demonstrate that position PX5 of the CXXXX$_5$XR P loop is critical to direct substrate selectivity either to pArg (PX5 = Thr) or pTyr (PX5 = Ile) and thus to determine, in combination with the depth of the active site, the substrate specificity of the LMW-PTPs and most probably also that of other protein phosphatase families (Figure 5).

To test this prediction, we performed a bioinformatic search for potential eukaryotic PAPs containing a PX5 threonine residue. In this search, we identified CG31469 of *Drosophila melanogaster*, a so-far-uncharacterized protein showing an age-dependent expression pattern (Lai et al., 2007), as fitting candidate (Figure S3). We then analyzed the activity of the putative phosphatase against different phospho-peptides. Remarkably, CG31469 exhibits substantial pArg phosphatase activity (Figure 4E), whereas it fails to dephosphorylate other substrates. Moreover, the Thr → Ile mutant (T11I) showed a similar effect in changing substrate specificity as observed for the bacterial PAP YwlE (Figure 4E; Table S2). Compared to the wild-type enzyme, the pArg phosphatase activity of CG31469 T11I was diminished 35-fold, whereas the activity against pTyr was improved 20-fold. Although we cannot exclude that this *Drosophila* phosphatase also dephosphorylates nonprotein substrates, the robust activity toward pArg-containing peptide implies that CG31469 acts in vivo as a bona fide PAP.

DISCUSSION

Owing to technical difficulties in working with phospho-arginine peptides (Schmidt et al., 2013), little is known about their functional and biological relevance as posttranslational protein modifiers. So far, it has been shown that McsB is a bacterial protein arginine kinase that exclusively targets arginine residues (Fuhrmann et al., 2009). In addition, a recent phospho-arginine proteome analysis revealed a number of arginine phosphorylated proteins in *B. subtilis* (Elsholz et al., 2012). Together these data demonstrate that arginine phosphorylation represents an

important posttranslational protein modification in Gram-positive bacteria. In this work, we show that the McsB-mediated phosphorylation can be directly reversed by YwlE, which is the founding member of the PAP phosphatase family targeting pArg residues with high specificity. The close interplay of YwlE and McsB is also evidenced by previous findings showing that YwlE influences the localization of McsB-regulated proteins in the cell (Hahn et al., 2009), functions as "inhibitor" of McsB (Elsholz et al., 2011) and is involved in the bacterial stress response (Musumeci et al., 2005). Moreover, our study reveals that the dephosphorylation of pArg residues by YwlE is a clearly defined enzymatic activity that is not shared by other protein phosphatases. To ensure substrate selectivity, YwlE encompasses a dual selectivity filter comprising a deep active-site pocket that has a polar belt at its bottom. This construction is perfectly suited to specifically accommodate phospho-arginine residues while discriminating the small pSer/pThr phospho-residues (filter: size) as well as the hydrophobic pTyr (filter: polarity) (Figure 5). The efficient hydrolysis of phospho-arginine is accomplished by selective recognition of the pArg guanidinium group that is recognized and oriented for catalysis by Asp118 and Thr11, the PX5 residue. Comparison of YwlE with related PTPs indicates that the exchange of isoleucine to threonine at the PX5 position is critical to evolve the PAP activity, a finding that led to the discovery of a YwlE homolog in *D. melanogaster*. We thus suppose that the dephosphorylation mechanism outlined for the bacterial YwlE enzyme may be conserved in other eukaryotic protein phosphatases as well, which are known to occur in great diversity. Among the many different types of phosphatases and pseudophosphatases are several proteins that could not be classified according to activity and thus represent attractive targets to screen for potential PAP activity. Moreover, the presence of a putative eukaryotic PAP suggests that protein arginine phosphorylation constitutes a widespread protein modification that may have been underestimated so far. To this regard, the crystal structure of the YwlE reaction intermediate provides an excellent basis to develop highly specific PAP inhibitors. Such inhibitors should be essential to monitor arginine-phosphorylated proteins in eukaryotic cells and evaluate the previously proposed impact of arginine phosphorylation for transcriptional regulation, epigenetics (Wakim and Aswad, 1994), and other fundamental biological processes.

EXPERIMENTAL PROCEDURES

The detailed description of experimental procedures is available online in the Supplemental Information.

Protein Expression and Purification

For functional studies, all phosphatase constructs were overexpressed in *Escherichia coli* BL21(DE3) cells. Protein purification was proceeded by Ni-NTA affinity and size-exclusion chromatography (SEC). Structural integrity of the proteins was validated by analytical SEC, dynamic light scattering, and circular dichroism measurements. For structural studies, YwlE from *B. subtilis* was expressed in the methionine auxotrophic *E. coli* cell line B834.

Generation of pArg-Specific Antibody

A pArg-specific antibody was generated in a phage-display screen (synthetic HuCAL PLATINUM library, Morphosys; Prassler et al., 2011) using a branched arginine phosphorylated peptide (KIVQSKpRGGGGYIK)$_2$KC derived from the CtsR protein. To obtain pArg-specific phages, primary hits were counterselected against closely related antigenic peptides that either were unphosphorylated or contained a pTyr residue instead of the pArg. The pArg-specific binders were sequenced and subcloned into human $F_{(ab)2}$ antibody format. Subsequently, the generated antibodies were tested for pArg selectivity using dot-blot analysis.

ELISA Screen for the Identification of Potential pArg Phosphatases

To pinpoint endogenous arginine phosphatases in *B. subtilis*, we developed a specific ELISA screen. In this screen, the pArg-specific antibody was instrumental to monitor the dephosphorylation of a pArg-containing protein (McsB-P) in the presence of various *B. subtilis* cell extracts. A secondary antibody (anti-human $F_{(ab')2}$-specific) conjugated with horseradish peroxidase was applied to quantify the bound pArg antibody, and thus the phospho-mark.

Characterization of the pArg Phosphatase Activity

To monitor the effect of different phosphatases on arginine phosphorylated CtsR (CtsR-P), different biochemical assays were carried out. First, phosphatase activity was evaluated by monitoring the dephosphorylation of radioactively (γ-^{32}P) labeled CtsR-P. Second, the counteracting effect of various phosphatases in restoring the DNA-binding capability of CtsR was tested in EMSA. Phosphatase activity against KpXSGGGYIKIIKV phospho-peptides was determined by the EnzCheck Phosphate assay (Invitrogen). In parallel, phosphatase activity was tested against pNPP following standard procedures.

Crystallization and Structure Solution of YwlE and YwlE$_{C7S}$

All YwlE crystals were grown with the sitting-drop vapor diffusion method in 96-well plates at 19°C. The YwlE crystals belonged to space group *C2* containing one YwlE molecule per asymmetric unit. For structure solution, a single wavelength anomalous dispersion (SAD) data set was collected at the Swiss Light Source (SLS, Beamline X06SA) at λ = 0.9791 Å using a Pilatus detector (Dectris). The C7S mutant of YwlE was crystallized after preincubation with 10 mM pArg. The structure of the C7S mutant was solved by molecular replacement at 1.8 Å resolution with diffraction data collected at the European Synchrotron Radiation Facility (ESRF, Grenoble, beamline ID 14-4). Data collection, phasing, and refinement statistics are summarized in Table S1. For further details, please refer to Extended Experimental Procedures.

ACCESSION NUMBERS

The Protein Data Bank accession numbers for the YwlE and YwlEC7S crystal structures are 4KK3 and 4KK4, respectively.

SUPPLEMENTAL INFORMATION

Supplemental Information includes Extended Experimental Procedures, three figures, and two tables and can be found with this article online at http://dx.doi.org/10.1016/j.celrep.2013.05.023.

LICENSING INFORMATION

ACKNOWLEDGMENTS

J.F. and T.C. designed the research; J.F., B.M., S.S., D.B.T., and A.L. performed the research; J.F., B.M., S.S., D.B.T, A.L., E.C., and T.C. analyzed data; J.F. and T.C. wrote the paper. We thank Kazuo Kobayashi for providing the *B. subtilis* phosphatase mutant strains, Karl Mechtler, Andreas Schmidt, and Matthias Madalinsky for preparing the pArg peptide used for antibody generation, and the beamline scientists at the ESRF and SLS and Dirk Reinert (Boehringer Ingelheim) for their support in collecting diffraction data. The

Research Institute of Molecular Pathology (IMP) is funded by Boehringer Ingelheim.

Received: April 15, 2013
Revised: May 7, 2013
Accepted: May 10, 2013
Published: June 13, 2013

REFERENCES

Barford, D., Das, A.K., and Egloff, M.P. (1998). The structure and mechanism of protein phosphatases: insights into catalysis and regulation. Annu. Rev. Biophys. Biomol. Struct. *27*, 133–164.

Denu, J.M., and Dixon, J.E. (1998). Protein tyrosine phosphatases: mechanisms of catalysis and regulation. Curr. Opin. Chem. Biol. *2*, 633–641.

Elsholz, A.K., Hempel, K., Michalik, S., Gronau, K., Becher, D., Hecker, M., and Gerth, U. (2011). Activity control of the ClpC adaptor McsB in Bacillus subtilis. J. Bacteriol. *193*, 3887–3893.

Elsholz, A.K., Turgay, K., Michalik, S., Hessling, B., Gronau, K., Oertel, D., Mäder, U., Bernhardt, J., Becher, D., Hecker, M., and Gerth, U. (2012). Global impact of protein arginine phosphorylation on the physiology of Bacillus subtilis. Proc. Natl. Acad. Sci. USA *109*, 7451–7456.

Fuhrmann, J., Schmidt, A., Spiess, S., Lehner, A., Turgay, K., Mechtler, K., Charpentier, E., and Clausen, T. (2009). McsB is a protein arginine kinase that phosphorylates and inhibits the heat-shock regulator CtsR. Science *324*, 1323–1327.

Hahn, J., Kramer, N., Briley, K., Jr., and Dubnau, D. (2009). McsA and B mediate the delocalization of competence proteins from the cell poles of Bacillus subtilis. Mol. Microbiol. *72*, 202–215.

Hanks, S.K., and Hunter, T. (1995). Protein kinases 6. The eukaryotic protein kinase superfamily: kinase (catalytic) domain structure and classification. FASEB J. *9*, 576–596.

Hunter, T. (1995). Protein kinases and phosphatases: the yin and yang of protein phosphorylation and signaling. Cell *80*, 225–236.

Jia, Z., Barford, D., Flint, A.J., and Tonks, N.K. (1995). Structural basis for phosphotyrosine peptide recognition by protein tyrosine phosphatase 1B. Science *268*, 1754–1758.

Kim, S.J., Jeong, D.G., Yoon, T.S., Son, J.H., Cho, S.K., Ryu, S.E., and Kim, J.H. (2007). Crystal structure of human TMDP, a testis-specific dual specificity protein phosphatase: implications for substrate specificity. Proteins *66*, 239–245.

Kirstein, J., Zühlke, D., Gerth, U., Turgay, K., and Hecker, M. (2005). A tyrosine kinase and its activator control the activity of the CtsR heat shock repressor in B. subtilis. EMBO J. *24*, 3435–3445.

Klumpp, S., and Krieglstein, J. (2009). Reversible phosphorylation of histidine residues in proteins from vertebrates. Sci. Signal. *2*, pe13.

Lai, C.Q., Parnell, L.D., Lyman, R.F., Ordovas, J.M., and Mackay, T.F. (2007). Candidate genes affecting Drosophila life span identified by integrating microarray gene expression analysis and QTL mapping. Mech. Ageing Dev. *128*, 237–249.

Mijakovic, I., Musumeci, L., Tautz, L., Petranovic, D., Edwards, R.A., Jensen, P.R., Mustelin, T., Deutscher, J., and Bottini, N. (2005). In vitro characterization of the Bacillus subtilis protein tyrosine phosphatase YwqE. J. Bacteriol. *187*, 3384–3390.

Musumeci, L., Bongiorni, C., Tautz, L., Edwards, R.A., Osterman, A., Perego, M., Mustelin, T., and Bottini, N. (2005). Low-molecular-weight protein tyrosine phosphatases of Bacillus subtilis. J. Bacteriol. *187*, 4945–4956.

Olsen, J.V., Blagoev, B., Gnad, F., Macek, B., Kumar, C., Mortensen, P., and Mann, M. (2006). Global, in vivo, and site-specific phosphorylation dynamics in signaling networks. Cell *127*, 635–648.

Patterson, K.I., Brummer, T., O'Brien, P.M., and Daly, R.J. (2009). Dual-specificity phosphatases: critical regulators with diverse cellular targets. Biochem. J. *418*, 475–489.

Perego, M., Hanstein, C., Welsh, K.M., Djavakhishvili, T., Glaser, P., and Hoch, J.A. (1994). Multiple protein-aspartate phosphatases provide a mechanism for the integration of diverse signals in the control of development in B. subtilis. Cell *79*, 1047–1055.

Pereira, S.F., Goss, L., and Dworkin, J. (2011). Eukaryote-like serine/threonine kinases and phosphatases in bacteria. Microbiol. Mol. Biol. Rev. *75*, 192–212.

Prassler, J., Thiel, S., Pracht, C., Polzer, A., Peters, S., Bauer, M., Nörenberg, S., Stark, Y., Kölln, J., Popp, A., et al. (2011). HuCAL PLATINUM, a synthetic Fab library optimized for sequence diversity and superior performance in mammalian expression systems. J. Mol. Biol. *413*, 261–278.

Rigden, D.J. (2008). The histidine phosphatase superfamily: structure and function. Biochem. J. *409*, 333–348.

Sarmiento, M., Puius, Y.A., Vetter, S.W., Keng, Y.F., Wu, L., Zhao, Y., Lawrence, D.S., Almo, S.C., and Zhang, Z.Y. (2000). Structural basis of plasticity in protein tyrosine phosphatase 1B substrate recognition. Biochemistry *39*, 8171–8179.

Schmidt, A., Ammerer, G., and Mechtler, K. (2013). Studying the fragmentation behavior of peptides with arginine phosphorylation and its influence on phospho-site localization. Proteomics *13*, 945–954.

Sickmann, A., and Meyer, H.E. (2001). Phosphoamino acid analysis. Proteomics *1*, 200–206.

Stoker, A.W. (2005). Protein tyrosine phosphatases and signalling. J. Endocrinol. *185*, 19–33.

Sun, F., Ding, Y., Ji, Q., Liang, Z., Deng, X., Wong, C.C., Yi, C., Zhang, L., Xie, S., Alvarez, S., et al. (2012). Protein cysteine phosphorylation of SarA/MgrA family transcriptional regulators mediates bacterial virulence and antibiotic resistance. Proc. Natl. Acad. Sci. USA *109*, 15461–15466.

Vega, C., Chou, S., Engel, K., Harrell, M.E., Rajagopal, L., and Grundner, C. (2011). Structure and substrate recognition of the Staphylococcus aureus protein tyrosine phosphatase PtpA. J. Mol. Biol. *413*, 24–31.

Wakim, B.T., and Aswad, G.D. (1994). Ca(2+)-calmodulin-dependent phosphorylation of arginine in histone 3 by a nuclear kinase from mouse leukemia cells. J. Biol. Chem. *269*, 2722–2727.

Xu, H., Xia, B., and Jin, C. (2006). Solution structure of a low-molecular-weight protein tyrosine phosphatase from Bacillus subtilis. J. Bacteriol. *188*, 1509–1517.

Zabell, A.P., Schroff, A.D., Jr., Bain, B.E., Van Etten, R.L., Wiest, O., and Stauffacher, C.V. (2006). Crystal structure of the human B-form low molecular weight phosphotyrosyl phosphatase at 1.6-A resolution. J. Biol. Chem. *281*, 6520–6527.

Zhang, Z.Y. (2003). Mechanistic studies on protein tyrosine phosphatases. Prog. Nucleic Acid Res. Mol. Biol. *73*, 171–220.